2018

IMPACT OF PHOSPHOINOSITIDES ON REGULATION OF K-ATP BY ATP AND HYDROGEN SULFIDE

Tyler Hendon
Virginia Commonwealth University

IMPACT OF PHOSPHOINOSITIDES ON REGULATION

OF K_{ATP} BY ATP AND HYDROGEN SULFIDE

A thesis submitted in partial fulfillment of requirements for the degree of Master of Science at Virginia Commonwealth University.

by

Tyler Hendon, B.S. in Biochemistry, Florida State University, 2008

Director: Dr. Diomedes Logothetis, Professor, Department of Physiology and Biophysics at Virginia Commonwealth University (Formerly) / Department of Pharmaceutical Sciences at Northeastern University (Presently)

Virginia Commonwealth University
Richmond, Virginia
May, 2018

ACKNOWLEDGMENT

TABLE OF CONTENTS

CHAPTERS

LIST OF FIGURES

ABSTRACT

IMPACT OF PHOSPHOINOSITIDES ON REGULATION OF K_{ATP} BY ATP AND

HYDROGEN SULFIDE

Tyler Hendon, B.S. in Biochemistry

A thesis submitted in partial fulfillment of requirements for the degree of Master of Science at Virginia Commonwealth University.

Virginia Commonwealth University, 2018

Director: Dr. Diomedes Logothetis, Professor, Department of Physiology and Biophysics at Virginia Commonwealth University (Formerly) / Department of Pharmaceutical Sciences at Northeastern University (Presently)

Hydrogen sulfide (H_2S) reduces ischemia reperfusion (IR) injury by stimulating adenosine triphosphate (ATP) sensitive potassium channels (K_{ATP}) [1-5]. Demonstrating H_2S stimulation is unique to K_{ATP}, as other inwardly rectifying potassium (Kir) channels demonstrate inhibition or are unaffected [6]. We recently showed that H_2S inhibits Kir2 and Kir3 by decreasing channel sensitivity to phosphatidylinositol 4,5-bisphosphate ($PI(4,5)P_2$ or PIP_2) [6]. Here, we test the hypothesis that H_2S regulation of Kir6.2, a pore-forming subunit of the K_{ATP} channel, is also dependent on PIP_2. Using whole-cell patch-clamp we show that H_2S increases the activity of Kir6.2 channels expressed in HEK-293 cells. To study the mechanism, we modulated PIP_2 levels by expressing a light-

activated phosphatase, or by including high levels of a water-soluble PIP_2 analog in the patch pipette. The results suggest that H_2S augmentation of Kir6.2 channel activity is increased when PIP_2 levels are elevated.

INTRODUCTION

Sarcolemmal K$_{ATP}$ is comprised of four sulfonylurea receptor (SUR) subunits (SUR1, SUR2A, or SUR2B) surrounding four pore-forming Kir6 subunits (Kir6.1 or Kir6.2) (**Fig. 1**). Different subunit types are predominant depending on tissue type; for example, ventricular cardiac myocytes contain predominantly Kir6.2 and SUR2A, and pancreatic beta cells contain predominantly Kir6.2 and SUR1 [7, 8]. There are also nuclear [9] and mitochondrial forms of K$_{ATP}$ [10]. Experiments in pancreatic beta cells suggest that nuclear K$_{ATP}$ can be comprised of Kir6.2 and SUR1, and the channel is suggested to regulate gene transcription in times of metabolic stress [9]. The composition of mitochondrial K$_{ATP}$ is still debated, and some research suggests that they contain none of the Kir6 or SUR subunits found in sarcolemmal and nuclear K$_{ATP}$ [7, 9, 10, 11] - Kir1.2 [7] and Kir1.1b have been suggested as possible pore-forming subunits, as well as the possibility that instead of an SUR, they are in complexes with other proteins [11].

Kir6 is one of seven subfamilies of Kir channels found in humans. This family of channels is marked by a selectivity filter that makes them highly selective to potassium ions, as well as an intracellular block from magnesium ions and polyamines that promotes the inwardly rectifying characteristic of these channels [12]. These factors make these channels an important contributor to the resting membrane potential,

1

limiting the excitability of tissues that express them. All Kir channels are affected by several of the same factors, such as activation by phosphatidylinositol 4,5-bisphosphate (PI(4,5)P$_2$ or PIP$_2$) and inhibition by barium ions [13]. Kir6 is unique among Kir channels in that this subfamily shows inhibition of channel activity by ATP – a feature that makes it important for regulation of metabolically sensitive cells like pancreatic beta cells and cardiomyocytes [7].

Structural and functional details of K$_{ATP}$ channels have been explored through electrophysiology, Molecular Dynamics Simulations (MDS) [6], mutations [4-6], genetic analysis of disorders [8, 14, 15], animal models [16-17], biochemical assays [4, 18], and cryo-electron microscopy (cryo-EM) [19]. These investigations have elucidated a great deal about these channels and have facilitated treatments for disorders involving K$_{ATP}$. For example, the sulfonylurea glibenclamide is a widely prescribed medication for type 2 diabetes that inhibits K$_{ATP}$ currents upon binding to the sulfonylurea receptor 1 (SUR1) subunit of the K$_{ATP}$ channels in pancreatic beta cells. The resulting membrane depolarization opens voltage-dependent calcium channels, increasing intracellular calcium levels, thereby stimulating insulin release [14].

Historically seen as toxic, there are recently uncovered roles for endogenous hydrogen sulfide (H$_2$S) in areas such as synaptic activity [20], inflammation [21], insulin release [22], and tissue protection against IR injury [1-5], and it is now considered a gasotransmitter, like carbon monoxide and nitric oxide. Endogenous enzymatic production from cystathionine γ-lyase, cystathionine-β-synthase, and 3-mercaptopyruvate sulfurtransferase converts L-cysteine into H$_2$S [23]. Kir6 containing K$_{ATP}$ channels (**Fig. 1**) are particularly interesting in the context of Kir modification by

2

H₂S, as they demonstrate unique activation [6] and K_{ATP} channels are implicated in H₂S-mediated IR injury [1-5]. This potential for H₂S to reduce IR injury, by stimulating K_{ATP}, has the potential to help patients affected by ischemic infarct or during organ transplantation.

While mechanistic details are still being explored, it is thought that H₂S acts through several K_{ATP}-mediated mechanisms to mitigate this damage, including reduction of calcium ion influx through hyperpolarization of the membrane, relaxation of smooth muscle, suppression of glutamate-induced ROS production by preventing depolarization of the mitochondrial membrane [24] by activation of mitochondrial K_{ATP} [10]. Mechanisms of H₂S-mediated protection that do not necessarily involve the activation of K_{ATP} have also been evidenced, including upregulation of endothelial nitric oxide synthase, Nrf2 signaling, and mTORC2 phosphorylation of Akt1 [25]. However, several studies indicate that an active K_{ATP} channel is a critical component of ischemia preconditioning. For example, when it was blocked by glibenclamide [26], or when the predominant ventricular cardiac K_{ATP} was removed in the creation of Kir6.2$^{-/-}$ knockout mice (which is evidenced to not be a critical subunit of mitochondrial K_{ATP} [16, 27]), the benefits of ischemia preconditioning were "abolished" [16, 26]. Both overexpression of SUR2A and activation of K_{ATP} by pinacidil or other potassium channel openers, were also shown to mimic the effects of ischemia preconditioning [7].

H₂S modification of Kir channels has been proposed to occur by sulfhydration of cysteine residues [6, 23]. The activating effects of H₂S on Kir6.1 containing K_{ATP} were shown to be abolished by a Kir6.1-C43S mutation, providing a strong argument that this activation is reliant on the sulfhydration of C43 [5]. Also, a C42R mutation in Kir6.2 has

3

been tied to diabetes [15]. The C43 and C42 cysteine residues, in Kir6.1 and Kir6.2 pore-forming subunits, respectively, represent a highly conserved cysteine in other Kir channels, which is adjacent to the docking site for PIP_2 [28], a central Kir channel regulator [13], as well as the ATP regulatory site of Kir6.1 and 6.2 [19] (**Fig. 1**).

We have studied interactions between Kir channels and PIP_2, as well as modulatory factors, providing evidence that H_2S modification of various Kir channels changes the channel dependence on PIP_2, using different assays in oocytes and Chinese Hamster Ovary (CHO) cells, such as depletion of PIP_2 by wortmannin or a voltage-sensitive phosphatase, using a short-chain (dioctanoyl), water-soluble analog of PIP_2, DiC_8, and MDS. This research also showed that effects of NaHS (an H_2S donor) on other Kir channels changed how they interacted with PIP_2 [6]. Also, when expressed in oocytes, Kir6.2Δ36 (which lacks the endoplasmic reticulum (ER) retention sequence, allowing expression and membrane localization of the functional inwardly-rectifying potassium channel that is regulated by ATP and PIP_2, without an SUR [29]) shows activation by NaHS [6]. The actions of the gasotransmitter carbon monoxide on Kir2.2 and Kir2.3, which has been shown to act through modification of cysteine residues, like H_2S [30], has also been linked to modification of channel-PIP_2 dependence [31]. Since the activity of H_2S on Kir channels has been linked to channel/PIP_2 interactions by our research, including preliminary MDS research that suggests a link to PIP_2 affinity [6], along with links found in the research of others, and since preliminary experiments with K_{ATP} and Kir6.2Δ36 show that H_2S increased currents in these channels, I tested the hypothesis that the H_2S enhancement of the predominant ventricular sarcolemmal K_{ATP} pore-forming subunit, Kir6.2 [27], is dependent on PIP_2.

4

RESULTS

Characteristic Responses of ATP Regulated Kir6.2Δ36 Channels to 3 mM and 0.3 mM ATP in the Patch Pipette

In order to examine the impact of H_2S on Kir6.2, the pore-forming subunit of the K_{ATP} channel, the behavior of Kir6.2Δ36 transfected into HEK293 cells, in the absence of the H_2S donor NaHS, was first examined. As the activity of Kir6.2 channels is known to be sensitive to ATP, different concentrations of ATP were examined for effects on Kir6.2Δ36 currents to determine the ATP sensitivity of Kir6.2Δ36 in the environment relevant to these experiments (**Fig. 2-5**). Whole-cell patch-clamp was employed to assay the currents, and different concentrations of ATP were added to the internal solution of the patch pipette. Cells were studied in a solution (here called High-K^+) with potassium ion (K^+) concentrations symmetrical to the internal solution of the patch pipette. High-K^+ was perfused following perfusion by a solution with low, quasi-physiological, concentration of K^+ (here called Low-K^+), which was used to maintain cell health before the assay began. Guided by prior research from the lab responsible for the creation of Kir6.2Δ36 [29], I showed that while 3 mM ATP produced significant inhibition of High-K^+ activated inward currents (**Fig. 2 and 6**), including 0.3 mM ATP in the patch, resulted in a permissive environment in which the High-K^+ activated currents steadily increased in each of the ~10-minute runs (**Fig. 4 and 6**).

5

During these experiments Kir6.2Δ36, in my hands, showed the behavior anticipated for a Kir channel. Large currents under the conditions of GΩ level patch-clamp recording are indicative of successful membrane localization of Kir6.2Δ36 channels, in the absence of an SUR. When concentrations of K^+ were symmetrical on either side of the membrane (i.e. when in High-K^+), the inward currents were notably larger than the outward currents, as anticipated for an inwardly-rectifying potassium channel. Reversal potentials (E_{REV}) showed variation between runs and occasionally differed from values calculated using the Nernst equation. Deviations from anticipated E_{REV} (~ -85 mV in Low-K^+ and -1 mV in High-K^+) could have been due to a number of factors, such as the timing and rate of development of leak affecting the permeability of ions and the relevance of using barium-subtracted currents to determine E_{REV} when the solution is in High-K^+ (such currents being determined by data found during the steady-state of barium-blocked currents as measured at the end of the ~10-minute experiments, and therefore do not necessarily reflect Kir-specific currents at earlier times, as the degree of leak is prone to change), as well as variable biological factors like the presence and activity of other channels. As the barium solution is in High-K^+, Low-K^+ currents could not be meaningfully barium-subtracted, meaning they were not necessarily Kir-specific, further reducing their utility in accurately determining E_{REV}. However, it was consistently demonstrated that the voltage at which the currents were equal to zero would continuously right-shift to more positive values, until approximately the same point in the time courses where the inflection points mark the end of precipitous activation by High-K^+ (**Fig. 3 and 5**). These points are marked in **Figures 2 and 4** as $E_{REV} \approx 0$. After this point, consistent with the cell remaining in symmetrical K^+

6

conditions, E_{REV} remained relatively stable. Finally, the inhibition of inward currents observed following the start of perfusion of a Ba^{2+} containing solution is also a hallmark of Kir channels, allowing for the determination of currents specific to Kir channels [13] (**Fig. 2-5**).

To quantify the relative effects of 3 mM and 0.3 mM ATP in the patch pipette, first, a percent inhibition from the maximum inward current (I_{MAX}) to the currents averaged over the 11 sec period before the start of perfusion by the barium solution was calculated for each of the cells studied (by a high-quality whole-cell patch-clamp recording). The latter time point was chosen as perfusion by the barium containing solution was not started until a steady-state had been reached, or in the case of runs examining the effects of 0.3 mM ATP alone, until sufficient time had passed (i.e. ~10 minutes) to allow for comparison to other assays utilizing 0.3 mM ATP. As currents being activated by 0.3 mM ATP would continue to activate after the time marking the start of barium perfusion until sufficient barium concentrations were reached to inhibit the channels, any I_{MAX} values occurring after this time period were excluded. All currents for this and other assays were calculated by averaging the currents from approximately 85 to 100 ms into each sweep in order to analyze the inward currents, free from any voltage-dependent effects occurring as a result of the immediate transition from 0 to -120 mV. Unless otherwise indicated (e.g. by the phrase "raw currents"), the currents analyzed are all also barium-subtracted - meaning that the average of currents over 11 sec during steady-state inhibition by the barium solution was measured for each run and subtracted from the raw currents in that run, in order to limit the analysis to Kir-

specific currents. Currents shown for representative time courses and voltage-ramp sweeps are raw currents.

The resulting average of the 3 mM ATP percent inhibitions of the Kir6.2Δ36 channel currents was 67% +/- 12% (SEM), n = 5, p = 0.003. Also, in accordance to the findings of Tucker et al. [29], we found that in my hands 0.3 mM ATP in the patch pipette created a permissive environment for High-K$^+$ activated currents, which gradually increased over each of the ~10-minute experiments analyzed. Correspondingly, the average percent inhibition from I_{MAX} with 0.3 mM ATP, calculated as for 3 mM ATP, was found to not be statistically different than 0% (9.6% +/- 4.4% (SEM), n = 6, p = 0.084). As anticipated, the average percent inhibition from I_{MAX} for 3 mM was significantly greater than that calculated for 0.3 mM ATP (p = 0.003) (**Fig. 6**). As one would anticipate from the steady activation by 0.3 mM ATP (**Fig. 4**), these times for I_{MAX} would occur shortly before the analyzed period before barium inhibition, often corresponding to a transient spike in currents from mechanical and biological noise (an average of 25 sec +/- 5 sec (SEM) before), while I_{MAX} from 3 mM ATP runs of approximately the same length (~10 min before perfusion of the barium solution) would take place an average of 375 sec +/- 64 sec (SEM) before, and would correspond to a clear inflection point in the time courses for inward currents, which we interpret as a reflection of sufficient exogenous ATP diffusing into the cell, from the pipette, to inhibit Kir6.2Δ36 (**Fig. 2**).

These results demonstrate that the behavior of Kir6.2Δ36 shown by Tucker et al. [29], could be consistently replicated in my hands. With this empirical confirmation of the utility of the experimental conditions with 0.3 mM ATP in the patch pipette, it was decided to proceed with experiments attempting to alter Kir6.2Δ36 currents by

8

manipulating PIP$_2$ levels in the cell. First, we aimed to inhibit currents by the depletion of PIP$_2$ through a light-sensitive phosphatase system pioneered by Hille and De Camilli et al [32].

5-ptase + CIBN-CAAX Light-Stimulation Showing Large Inhibition of Kir2.3 Currents

The light-activated phosphatase system used is comprised of two fusion proteins: CRY2-5-ptase$_{OCRL}$ contains the photolyase domain of cyrptochrome 2 (CRY2) and the inositol 5-phosphatase domain of the Lowe oculocerbrorenal syndrome protein (OCRL), while CIBN-CAAX contains the CRY2 binding domain (CIBN) and a C-terminal CAAX box for plasma membrane targeting. When CRY2-5-ptase$_{OCRL}$ and CIBN-CAAX fusion proteins are co-expressed and exposed to light between 458-488 nm, the 5-ptase is localized to the plasma membrane, where it dephosphorylates PIP$_2$. The utility of this system to study the PIP$_2$ dependence of ion channel activity was demonstrated by the Hille and De Camilli labs. Within seconds of light-stimulation, they observed the inhibition of KCNQ2/3 channel currents corresponding to the rapid dephosphorylation of the 5-phosphates of PIP$_2$, as well as PI(3,4,5)P$_3$ [32].

I used Kir2.3 as a positive control to demonstrate that the light-sensitive phosphatase system worked in my hands, since unpublished data in the lab by Plant et al. had previously shown it to inhibit this channel in whole-cell patch-clamp. Also, Kir2.3 is activated by PIP$_2$ to a similar degree as Kir6.2 [33], and Kir6.2 has been shown to possess a similar affinity for PIP$_2$ as Kir6.2Δ36 [18].

9

In my hands, the activation of the phosphatase significantly inhibited Kir2.3 currents by an average of 79% +/- 4.3% (SEM), n = 6, p < 0.001, as calculated by comparing the average of currents over the 11 sec before exposing the cells to 460 nm light, to the 11 sec average before the start of perfusion by the barium containing solution (**Fig. 9**). The inhibition began within a few seconds, as shown in the representative time course in **Figure 7**, consistent with previous research [32]. Once the inhibition reached steady-state, allowing for the percent change in currents to be calculated, the perfusion of the barium containing solution would begin.

5-ptase + CIBN-CAAX Light-Stimulation Shows No Discernible Inhibition of Kir6.2Δ36 Currents

After approximately thirty attempts to adjust conditions, and to maximize likelihood that vectors were successfully transfected into the cell being examined, it became clear that activation of the light-sensitive phosphatase resulted in no observable change in Kir6.2Δ36 currents during the same time course observed in experiments with convincing Kir2.3 inhibition (**Fig. 7-9**). From these attempts, 13 were found to be of high enough quality to include in analysis. The analysis of these runs, performed as described for Kir2.3, showed that the currents did not significantly change from the time before the point of light-stimulation to the time before perfusion by the barium solution (average percent change = +13% +/- 9.4% (SEM), n = 13, p = 0.189). Since this is significantly different from the average percent change with Kir2.3 under similar conditions (p < 0.001) (**Fig. 9**), and the channels were anticipated to behave

10

similarly due to their similar affinity for PIP_2, we felt that further analysis of this disparity was warranted.

Effects of 0.3 mM ATP in the Patch Pipette on Kir6.2Δ36 Current, with and without 5-ptase + CIBN-CAAX

To further analyze the unanticipated behavior of the light-sensitive phosphatase system on Kir6.2Δ36, a comparison was made between when the system was present and when it wasn't (**Fig. 10**), using the same 0.3 mM ATP data generated to compare the effects of 0.3 and 3 mM ATP, in the patch pipette, on the channel (**Fig. 4-6**). To further illustrate this unanticipated behavior, a figure was included to show the averages of raw currents over the 11 sec before light-stimulation, and the 11 sec before the perfusion by the barium solution, for the run made in the presence of the 5-ptase system (**Fig. 10A**). For comparison, the same presentation is made for data generated without the system present, and since no times of light-stimulation correspond to these data, and the length of between the relevant time points is approximately equal whether or not the system is present, the average time of light-stimulation for the Kir6.2Δ36 data for which the system was present (t = 146 sec) was used in place of the time of light-stimulation for the data in which it was not (**Fig 10B**).

Determination of the average of percent changes from runs with the 5-ptase system was performed as described for **Figure 9**, which also shows the result of +13% +/- 9.4% (SEM), n = 13. For data in which the system was not present, this analysis was performed by using the t = 146 sec average in place of the starting time of light-stimulation, and the average of percent changes from the average of currents over 11

11

sec before that point to the average of currents over 11 sec before the start of perfusion by the barium solution was found to be +190% +/- 59% (SEM), n = 6, p = 0.011. This anticipated activation by the permissive environment of 0.3 mM ATP was found to be significantly muted when in the presence of the light-stimulated phosphatase system (p-value = 0.001) (**Fig. 10C**), even though no observable rapid change was triggered by light-stimulation taking place (**Fig. 8**). The potential mechanisms of this long-term impact are detailed in the "Discussion" section. However, as the effects of the system were not the rapid inhibition of currents by the depletion of PIP_2 that was anticipated, a more direct manipulation of PIP_2 levels was employed by using a water-soluble analog of PIP_2, DiC_8, in order to examine the resulting impact of increasing levels of PIP_2 on Kir6.2Δ36 activation by NaHS.

Average Percent Change of Kir6.2Δ36 Currents by Perfusion of 3 mM NaHS with and without 0.2 mM DiC₈ in the Patch Pipette

A patch pipette concentration of DiC_8 in whole-cell patch-clamp experiments of 0.2 mM DiC_8 has been shown previously by our lab to be both viable and near the upper end of what has been shown to facilitate assayable differences in currents [34]. Consequently, it was decided to use this concentration to look for changes in the degree of activation of Kir6.2Δ36 currents by NaHS.

Our previous experiments in oocytes showing inhibition of Kir3.2* currents and activation of Kir6.2Δ36 currents by incubating the oocytes in 2 mM NaHS solution for over 100 minutes, demonstrated significantly diminished regulation with shorter

incubation periods [6]. In contrast, I was able to see activation of Kir6.2Δ36 currents from 3 mM NaHS in HEK293 cells begin within a few seconds and reach steady-state within ~10 minutes (**Fig. 11 and 12**). The data were analyzed in the same manner used to determine the average percent change from the light-stimulation of the phosphatase system, except that instead of the time of light-stimulation the start of the perfusion by the NaHS solution was used. Resulting data was used to compare the average percent activation of Kir6.2Δ36 currents by NaHS for when 0.2 mM DiC_8 was present in the patch pipette to when it was not.

The average percent activation by NaHS when DiC_8 was not present was 370% +/- 120% (SEM), n = 6, p = 0.013. With 0.2 mM DiC_8 in the patch pipette the average percent activation was 530% +/- 120% (SEM), n = 6, p = 0.003. While the percent activation in the presence of 0.2 mM DiC_8 does not indicate significance within the constraints of a 95% confidence interval (p = 0.087), the data do seem to indicate a trend that might reach significance with further experimentation.

DISCUSSION

In examining the ATP sensitivity of Kir6.2Δ36, I found that 0.3 mM ATP in the patch pipette allowed for stable High-K$^+$ activated currents, suitable for analysis by further manipulation. Next, as attempts to utilize a light-sensitive phosphatase system under these conditions did not yield a demonstrable, rapid inhibition of currents that could be tied to PIP$_2$ reduction, experiments involving the addition of DiC$_8$ to the patch pipette were carried out. Finally, under the conditions suggested by these experiments, the hypothesis that activation of Kir6.2 by H$_2$S is dependent on PIP$_2$ was tested. I found that in experimental conditions with additional PIP$_2$ (in the form of DiC$_8$) introduced into the cells, the effects of H$_2$S donor NaHS was increased, showing a nearly statistically significant trend ($p = 0.087$). It is possible that a larger set of experiments would show statistical significance. Although limited in scope, these findings may help widen the body of knowledge associated with K$_{ATP}$ regulation, and hopefully contribute towards the development of treatments less deleterious than H$_2$S ischemia preconditioning. By providing information about Kir channel/PIP$_2$ interactions, and how they can be manipulated, it may also help to elucidate other Kir related medical conditions, particularly those associated with Kir6.2, such as diabetes.

Initial whole-cell patch-clamp experiments focused on determining the applicability, in my hands, of research performed by Tucker et al. [29] (the first lab to

14

report using Kir6.2Δ36). Specifically, to see if their findings that, while 3 mM ATP in the patch-pipette would be inhibitory, 0.3 mM ATP would allow for Kir6.2Δ36 currents large enough to allow for assaying modulation by other channel regulators. I found their research to be reproducible, and that activation by including 0.3 mM ATP in the patch pipette provided a stable environment in which I could perform my planned experiments. While using 0 mM ATP could be considered for activating an ATP-inhibited channel like this one, these conditions were rejected to allow for the general health of the cell over a several minute whole-cell patch-clamp experiment, already involving unfavorable conditions like higher than physiological concentrations of K^+, and to allow for the endogenous synthesis of PIP_2 and other relevant phosphoinositides.

When it was discovered that the light-sensitive phosphatase system, which worked as anticipated in my hands and those of others for Kir2.3, was not demonstrating discernible inhibition of Kir6.2Δ36 currents within seconds of light-stimulation, but did appear to have a significant long-term impact, an investigation was begun into previous research for reasons why that may be the case. First, I found that our own lab's investigations of how phosphoinositides effect Kir channels had shown that Kir6.2 containing K_{ATP} and Kir6.2Δ36 channels were activated by a greater range of phosphoinositides than Kir2.3, as well as other Kir channels investigated [35]. However, the study did not explicitly test the effects of PI(4)P, which is generated 1:1 by the depletion of $PI(4,5)P_2$ by the 5-phosphatase I employed here. While the levels of other phosphoinositides would also be affected, namely depletion of $PI(3,4,5)P_3$ into $PI(3,4)P_2$, the impact of these changes on Kir6.2Δ36 currents are likely to be negligible, even though Kir6.2Δ36 shows activation from each comparable to $PI(4,5)P_2$ [35],

15

because i) they are present in HEK-293 cells at relatively low levels [36], and ii) the depletion of PI(3,4,5)P$_3$ creates the PI(3,4)P$_2$ 1:1, and their degree of activation of the Kir6.2Δ36 is approximately equal [35].

Further investigation into past research revealed that when a voltage-sensitive 5-phosphatase was used to deplete PI(4,5)P$_2$, while causing inhibition of Kir2.1, Kv7.2, and Kv7.3, it had virtually no effect on K$_{ATP}$ comprised of Kir6.2 and SUR1. Hypothesizing that the PI(4)P created by this phosphatase was activating K$_{ATP}$ to a similar degree as PI(4,5)P$_2$, the authors then used direct application, to excised patches after run-down of endogenous phosphoinositides, of either PI(4,5)P$_2$ or PI(4)P to show that, while only PI(4,5)P$_2$ activated Kir2.1, both PI(4,5)P$_2$ and PI(4)P "similarly activated Kir6.2/SUR1." As their experiments generally took place in under 200 sec, long-term effects like those I observed were not analyzable [37].

Furthermore, to explore possible relevant differences in affinity of phosphoinositides in Kir6.2 containing K$_{ATP}$ channels versus Kir6.2Δ36, Wang and colleagues used a dot-blot assay with Kir6.2Δ35 against several phosphoinositides, evidencing a similar binding efficiency for PI(4,5)P$_2$ and PI(4)P [18].

Convinced by my own empirical data and support of the cited literature, we feel it is likely that the light-sensitive phosphatase system did not produce the anticipated inhibition of currents within seconds of light-stimulation because PI(4)P is approximately as effective as PI(4,5)P$_2$ in activating Kir6.2Δ36 channels, and was being generated at the same rate of the depletion of PI(4,5)P$_2$. The significant difference found over longer time periods after light-stimulation of the phosphatase system, as compared to 0.3 mM ATP alone, could be due to multiple factors. Possibilities include i) the potential of

16

PI(4)P to have a lower affinity than PIP$_2$ for Kir6.2Δ36 (although, if the hypothesis is correct that the depletion of PIP$_2$ did not have any observable, rapid impact on currents because of its replacement with PI(4)P, then we would also hypothesize that any effects on currents due to PI(4)P/channel affinity would be as rapidly apparent as the effect of the depletion of PIP$_2$ on other channels), ii) unrelated effects of PIP$_2$ depletion or PI(4)P generation on cellular metabolism, and iii) the effects of PI(4)P, as compared to PIP$_2$, on the proximate ATP binding pocket. In support of the latter hypothesis, phosphoinositides have been evidenced to directly impact the affinity of ATP for Kir6.2Δ35 [18], and as the effect currents by the light-stimulation of the phosphatase were slow, the correlation to the rate of change of currents caused by the dilution of cellular ATP from having 0.3 mM ATP in the patch pipette may indicate a causal relationship.

While it could still be informative to test for the PIP$_2$ dependent effects of H$_2$S activation of K$_{ATP}$ currents by investigating for potential differential dependence on PI(4,5)P$_2$ versus PI(4)P, given the limited scope of this Master's thesis work, we decided to investigate this potential PIP$_2$ dependence through more direct means - by comparing the effects of the H$_2$S donor NaHS between the endogenous levels of PIP$_2$ and increased PIP$_2$ levels, through the inclusion of its water-soluble analog (DiC$_8$), in the patch pipette.

This method allowed for the investigation of the central hypothesis, that H$_2$S activation of Kir6.2 currents is dependent on PIP$_2$. To this end, comparisons were made between endogenous levels of PIP$_2$ and conditions in which additional short-chain PIP$_2$ was added through the patch pipette, with the expectation that endogenous PIP$_2$

would predominantly remain in the lipid membrane, and the amount lost during equilibrium with the internal solution of the patch pipette would remain approximately consistent between these conditions. It was found that, when in the presence of additional short-chain PIP_2, the average percent activation of currents by NaHS was higher (530% +/- 120% (SEM), n = 6, p = 0.013) than without DiC_8 (340% +/- 120% (SEM), n = 6, p = 0.003). Falling between a 90-95% confidence interval (p = 0.087), the statistical significance of this difference in average percent activation by NaHS suggests that increased levels of PIP_2 would facilitate H_2S activation of Kir6.2. The statistical analysis of this, and all other statistical analysis in this paper, is limited by the number of repetitions of each experiment. As such, it is possible that additional repetition would increase the statistical significance to above the 95% confidence interval.

The goal of this research is to further the understanding of K_{ATP} channels and the interaction of regulatory factors, particularly ATP, PIP_2, and H_2S, in order to facilitate the development of medical therapies. Since these findings are limited to Kir6.2Δ36, instead of the complete K_{ATP} channel, the medical applicability of these findings may be limited by the absence of the regulatory SUR subunits, which have also been demonstrated to be directly modified by H_2S [4]. However, as I demonstrate that my experimental conditions still involve a functional inwardly-rectifying potassium channel that demonstrates regulation by ATP, PIP_2, and H_2S, the information gained may still be quite valuable.

As H_2S is known to affect many important biological processes [1-6, 20-23, 25, 30], its medical application for targeted effects, such as activating sarcolemmal K_{ATP} in ventricular cardiac myocytes to reduce IR injury, is bound to have considerable off-

target effects. Indeed, it has been shown that H_2S preconditioning, while cardioprotective, actually furthers neuronal damage during IR. The exact cause is still being investigated, but it has been shown that H_2S has a depolarizing effect on neuronal tissue, instead of the hyperpolarizing effect it has on cardiac tissue [38]. This may be due to the fact that it inhibits many Kir channels, and this effect could overwhelm the effects of neuronal Kir6 channels being activated [6] - investigations into the relative expression patterns and corresponding contributions from inhibition or activation of Kir channels in specific neurons could help our understanding in this matter. The more we understand about these concepts, the better chance we have for developing a more focused therapy, such as a Kir6.2 or cardiac tissue specific treatment that quickly increases Kir channel-PIP_2 interactions.

In conclusion, my patch-clamp studies using Kir6.2Δ36 are consistent with our previous work on Kir2 and Kir3 channels in that the H_2S effects on these channels suggest dependence on phosphoinositides. H_2S modulation under high PIP_2 level conditions suggest an augmented activation of Kir6.2Δ36 currents. Presumably the availability of increased PIP_2 in the inner leaflet of the plasma membrane allowed for enhanced interactions by H_2S post-translational modifications.

MATERIALS AND METHODS

Materials – Dioctanoyl PIP$_2$ (DiC$_8$) was purchased from Echelon (Salt Lake, UT). It was dissolved in water in 6 mM stock solution aliquots and stored at -80°C. On the day of the experiment it was diluted in the intracellular solution to a concentration of 0.2 mM. NaHS was purchased from Strem (Newburyport, MA) and on the day of experiments it was dissolved into the High-K$^+$ solution to a concentration of 3 mM.

Molecular Biology – Kir2.3 was handled in pcDNA and eGFP was handled in peGFP-C1. Kir6.2Δ36 was subcloned from pGEM-HE (as used by Ha et al. [6]) to pXoom, a plasmid with a CMV promoter for expression in mammalian cells. CRY2-5-ptase$_{OCRL}$ and CIBN-CAAX were gifted from the De Camilli lab in mammalian expression vectors under the control of CMV promoters [32].

Electrophysiology – Whole-cell currents were measured by conventional patch-clamp with an Axopatch 200B amplifier (Molecular Devices) controlled via a USB-interface (National Instruments) using WinWCP software (University of Strathclyde). In all cases, currents were acquired through a lowpass Bessel filter at 2 kHz and were digitized at 10 kHz. Patch pipettes were fabricated using a Narishige PC-10 puller and had a resistance of around 6 MΩ when filled with an intracellular solution comprising: 140 mM KCl, 2 mM MgCl$_2$, 1 mM EGTA, 0.3 or 3 mM Na$_2$ATP, 0.1 mM Na$_2$GTP, and 5 mM HEPES; pH = 7.2. Cells for study were selected based on eGFP expression using

an epifluorescence microscope (Nikon). To study Kir channel currents, cells were held at 0 mV, and currents were assessed by ramps from -120 to +80 mV (as shown and described in **Figure 3**). Cells were perfused via a multi-channel gravity-driven perfusion manifold, with the Low-K$^+$ solution, then quickly transitioning to the High-K$^+$ solution (at ~10 s). The barium solution was perfused at the end of each run to determine the magnitude of the barium-sensitive currents. The High-K$^+$ solution comprised: 5 mM NaCl, 135 mM KCl, 1.2 mM MgCl$_2$, 1.5 mM CaCl$_2$, 8 mM Glucose, and 10 mM HEPES; pH = 7.4. The Low-K$^+$ solution comprised: 135 mM NaCl, 5 mM KCl, 1.2 mM MgCl$_2$, 1.5 mM CaCl$_2$, 8 mM Glucose, and 10 mM HEPES; pH = 7.4. Barium was used at 3 mM BaCl$_2$ in the High-K$^+$ solution. Barium sensitive currents were defined as the difference between the steady-state currents while cells were perfused by High-K+ and barium-containing solutions.

Because H$_2$S can interact with the silver chloride that forms the ground electrodes used, patch-clamp studies were performed using a salt bridge between the recording chamber and the ground wire. The salt bridge was formed by 1 M KCl solution soaked into 2% agarose and was housed in a 3 cm length of P160 tubing (Warner Instruments).

Currents were primarily analyzed in the range of 85 – 100 ms in each sweep to investigate inward currents. Light-stimulation was achieved using a 460 nm LED (Luminus PT-54-TE) that was focused on the cells through the objective lens of an inverted microscope (Nikon). Data acquisition and analysis was carried out using WinWCP V5.2.9, ClampFit 10.7 (Molecular Devices), and Microsoft Excel.

Culture of HEK-293-E Cells – Cells were maintained in DMEM supplemented with 10% FBS and 1% Penicillin Streptomycin (Hyclone). Plasmids were transfected into cells with Lipofectamine 2000 (ThermoFisher) or EcoTransfect (OzBiosciences) according to the manufacturer's instructions, in Opti-MEM (ThermoFisher). Cells were cultured in Corning 100 mm x 20 mm cell culture treated dishes until approximately 80% confluence. They were then trypsinized with 1 ml of 0.05% Trypsin (Hyclone), left to detach for ~3 minutes and diluted with 14 ml of the supplemented DMEM. Four glass cover-slips were coated with trypsinized cells in a BioLite 35 mm tissue culture dish (ThermoFisher) and allowed to attach over 10 minutes before the addition of 2 ml of supplemented DMEM. The next day, transfection was performed with 1 µg of Kir channel vector, 0.75 µg each of DNA for CRY2-5-ptase$_{OCRL}$ and CIBN-CAAX vectors, and 0.25 µg of eGFP vector. Cells were studied 24 hours later with eGFP fluorescence used as a marker of protein expression.

Data Analysis and Statistics – All data are reported as mean +/- Standard Error of the Mean (SEM); 'n' represents the number of cells assayed and included in the analysis for each condition. Average percent changes were calculated as described in the "Results" section and corresponding figure legends. The statistical significance of the data were assessed using the "Single Sample t-Test" and "Mann-Whitney Test" online calculators provided by Vassar College. Data were analyzed using one or two-tailed tests, as stated in the corresponding figure legends, based on the hypothesis under investigation. Data were analyzed as one-tailed if previous evidence suggested a direction of change, positive or negative – otherwise the analysis was two-tailed.

REFERENCES CITED

[1] Nicholson, C. K., & Calvert, J. W. (2010). Hydrogen sulfide and ischemia–reperfusion injury. *Pharmacological Research*, *62*(4), 289–297. https://doi.org/10.1016/j.phrs.2010.06.002

[2] Wang, R. (2011). Signaling pathways for the vascular effects of hydrogen sulfide: Current Opinion in Nephrology and Hypertension, 20(2), 107–112. https://doi.org/10.1097/MNH.0b013e3283430651

[3] Zhao, W., Zhang, J., Lu, Y., & Wang, R. (2001). The vasorelaxant effect of H_2S as a novel endogenous gaseous K_{ATP} channel opener. *The EMBO Journal*, *20*(21), 6008–6016. http://doi.org/10.1093/emboj/20.21.6008

[4] Kang M., Hashimoto A., Gade A., Akbarali H.I. (2015). Interaction between hydrogen sulfide-induced sulfhydration and tyrosine nitration in the K_{ATP} channel complex. Am. J. Physiol. Gastrointest. Liver Physiol. 2015;308:G532–G539. doi: 10.1152/ajpgi.00281.2014.

[5] Mustafa, A. K., Sikka, G., Gazi, S. K., Steppan, J., Jung, S. M., Bhunia, A. K., … Snyder, S. H. (2011). Hydrogen Sulfide as Endothelium-Derived Hyperpolarizing Factor Sulfhydrates Potassium Channels. *Circulation Research*, *109*(11), 1259–1268. https://doi.org/10.1161/CIRCRESAHA.111.240242

[6] Ha, J., Xu, Y., Kawano, T., Hendon, T., Baki, L., Garai, S., … Logothetis, D. E. (2018). Hydrogen sulfide inhibits Kir2 and Kir3 channels by decreasing sensitivity to the phospholipid phosphatidylinositol 4,5-bisphosphate (PIP_2). *Journal of Biological Chemistry*, *293*(10), 3546–3561. https://doi.org/10.1074/jbc.RA117.001679

[7] Tinker, A., Aziz, Q., & Thomas, A. (2014). The role of ATP-sensitive potassium channels in cellular function and protection in the cardiovascular system: ATP-sensitive K^+ channels. British Journal of Pharmacology, 171(1), 12–23. https://doi.org/10.1111/bph.12407

[8] Rorsman, P., & Ashcroft, F. M. (2018). Pancreatic β-Cell Electrical Activity and Insulin Secretion: Of Mice and Men. Physiological Reviews, 98(1), 117–214. https://doi.org/10.1152/physrev.00008.2017

[9] Quesada, I., Rovira, J. M., Martin, F., Roche, E., Nadal, A., & Soria, B. (2002). Nuclear KATP channels trigger nuclear Ca^{2+} transients that modulate nuclear function. Proceedings of the National Academy of Sciences, 99(14), 9544–9549. https://doi.org/10.1073/pnas.142039299

[10] Wojtovich, A. P., Urciuoli, W. R., Chatterjee, S., Fisher, A. B., Nehrke, K., & Brookes, P. S. (2013). Kir6.2 is not the mitochondrial KATP channel but is required for cardioprotection by ischemic preconditioning. American Journal of Physiology-Heart and Circulatory Physiology, 304(11), H1439–H1445. https://doi.org/10.1152/ajpheart.00972.2012

[11] Foster, D. B., Ho, A. S., Rucker, J., Garlid, A. O., Chen, L., Sidor, A., … O'Rourke, B. (2012). Mitochondrial ROMK Channel Is a Molecular Component of MitoKATP. Circulation Research, 111(4), 446–454. https://doi.org/10.1161/CIRCRESAHA.112.266445

[12] Oliver, D., Baukrowitz, T., & Fakler, B. (2000). Polyamines as gating molecules of inward-rectifier K^+ channels: Polyamines as gating molecules of Kir channels. European Journal of Biochemistry, 267(19), 5824–5829. https://doi.org/10.1046/j.1432-1327.2000.01669.x

[13] Tang, Q.-Y., Larry, T., Hendra, K., Yamamoto, E., Bell, J., Cui, M., … Boland, L. M. (2015). Mutations in Nature Conferred a High Affinity Phosphatidylinositol 4,5-Bisphosphate-binding Site in Vertebrate Inwardly Rectifying Potassium Channels. Journal of Biological Chemistry, 290(27), 16517–16529. https://doi.org/10.1074/jbc.M115.640409

[14] Ashcroft, F. M. (2005). ATP-sensitive potassium channelopathies: focus on insulin secretion. Journal of Clinical Investigation, 115(8), 2047–2058. https://doi.org/10.1172/JCI25495

[15] Yorifuji, T., Nagashima, K., Kurokawa, K., Kawai, M., Oishi, M., Akazawa, Y., … Nakahata, T. (2005). The C42R Mutation in the Kir6.2 (KCNJ11) Gene as a Cause of Transient Neonatal Diabetes, Childhood Diabetes, or Later-Onset, Apparently Type 2 Diabetes Mellitus. The Journal of Clinical Endocrinology & Metabolism, 90(6), 3174–3178. https://doi.org/10.1210/jc.2005-0096

[16] Suzuki, M., Sasaki, N., Miki, T., Sakamoto, N., Ohmoto-Sekine, Y., Tamagawa, M., … Nakaya, H. (2002). Role of sarcolemmal KATP channels in cardioprotection against ischemia/reperfusion injury in mice. Journal of Clinical Investigation, 109(4), 509–516. https://doi.org/10.1172/JCI14270

[17] Suzuki, M. (2003). Cardioprotective Effect of Diazoxide Is Mediated by Activation of Sarcolemmal but Not Mitochondrial ATP-Sensitive Potassium Channels in Mice. Circulation, 107(5), 682–685. https://doi.org/10.1161/01.CIR.0000055187.67365.81

[18] Wang, C., Wang, K., Wang, W., Cui, Y., & Fan, Z. (2002). Compromised ATP binding as a mechanism of phosphoinositide modulation of ATP-sensitive K$^+$ channels. FEBS Letters, 532(1–2), 177–182. https://doi.org/10.1016/S0014-5793(02)03671-2

[19] Martin, G. M., Yoshioka, C., Rex, E. A., Fay, J. F., Xie, Q., Whorton, M. R., … Shyng, S.-L. (2017). Cryo-EM structure of the ATP-sensitive potassium channel illuminates mechanisms of assembly and gating. ELife, 6. https://doi.org/10.7554/eLife.24149

[20] Abe, K., & Kimura, H. (1996). The possible role of hydrogen sulfide as an endogenous neuromodulator. *The Journal of Neuroscience: The Official Journal of the Society for Neuroscience*, *16*(3), 1066–1071.

[21] Li, L., Bhatia, M., Zhu, Y. Z., Zhu, Y. C., Ramnath, R. D., Wang, Z. J., … Moore, P. K. (2005). Hydrogen sulfide is a novel mediator of lipopolysaccharide-induced inflammation in the mouse. *FASEB Journal: Official Publication of the Federation of American Societies for Experimental Biology*, *19*(9), 1196–1198. https://doi.org/10.1096/fj.04-3583fje

[22] Kaneko, Y., Kimura, Y., Kimura, H., & Niki, I. (2006). L-cysteine inhibits insulin release from the pancreatic beta-cell: possible involvement of metabolic production of hydrogen sulfide, a novel gasotransmitter. *Diabetes*, *55*(5), 1391–1397.

[23] Paul, B. D., & Snyder, S. H. (2012). H$_2$S signaling through protein sulfhydration and beyond. *Nature Reviews. Molecular Cell Biology*, *13*(8), 499–507. https://doi.org/10.1038/nrm3391

[24] Shukry, M., Kamal, T., Ali, R., Farrag, F., Almadaly, E., Saleh, A. A., & Abu El-Magd, M. (2015). Pinacidil and levamisole prevent glutamate-induced death of hippocampal neuronal cells through reducing ROS production. Neurological Research, 37(10), 916–923. https://doi.org/10.1179/1743132815Y.0000000077

[25] Li, C., Hu, M., Wang, Y., Lu, H., Deng, J., & Yan, X. (2015). Hydrogen sulfide preconditioning protects against myocardial ischemia/reperfusion injury in rats through inhibition of endo/sarcoplasmic reticulum stress. International Journal of Clinical and Experimental Pathology, 8(7), 7740–7751.

[26] Gross, G. J., & Auchampach, J. A. (1992). Blockade of ATP-sensitive potassium channels prevents myocardial preconditioning in dogs. Circulation Research, 70(2), 223–233. https://doi.org/10.1161/01.RES.70.2.223

[27] Seharaseyon, J., Ohler, A., Sasaki, N., Fraser, H., Sato, T., Johns, D. C., … Marbán, E. (2000). Molecular Composition of Mitochondrial ATP-sensitive Potassium Channels Probed by Viral Kir Gene Transfer. Journal of Molecular and Cellular Cardiology, 32(11), 1923–1930. https://doi.org/10.1006/jmcc.2000.1226

[28] Lopes, C. M. B., Zhang, H., Rohacs, T., Jin, T., Yang, J., & Logothetis, D. E. (2002). Alterations in Conserved Kir Channel-PIP$_2$ Interactions Underlie Channelopathies. Neuron, 34(6), 933–944. https://doi.org/10.1016/S0896-6273(02)00725-0

[29] Tucker, S. J., Gribble, F. M., Zhao, C., Trapp, S., & Ashcroft, F. M. (1997). Truncation of Kir6.2 produces ATP-sensitive K$^+$ channels in the absence of the sulphonylurea receptor. *Nature*, *387*(6629), 179–183. https://doi.org/10.1038/387179a0

[30] Yang, G. (2017). Gasotransmitters and Protein Post-Translational Modifications. *MOJ Proteomics & Bioinformatics*, *5*(4). https://doi.org/10.15406/mojpb.2017.05.00165

[31] Liang, S., Wang, Q., Zhang, W., Zhang, H., Tan, S., Ahmed, A., & Gu, Y. (2014). Carbon monoxide inhibits inward rectifier potassium channels in cardiomyocytes. *Nature Communications*, *5*, 4676. https://doi.org/10.1038/ncomms5676

[32] Idevall-Hagren, O., Dickson, E. J., Hille, B., Toomre, D. K., & De Camilli, P. (2012). Optogenetic control of phosphoinositide metabolism. *Proceedings of the National Academy of Sciences*, *109*(35), E2316–E2323. https://doi.org/10.1073/pnas.1211305109

[33] Du, X., Zhang, H., Lopes, C., Mirshahi, T., Rohacs, T., & Logothetis, D. E. (2004). Characteristic Interactions with Phosphatidylinositol 4,5-Bisphosphate Determine Regulation of Kir Channels by Diverse Modulators. Journal of Biological Chemistry, 279(36), 37271–37281. https://doi.org/10.1074/jbc.M403413200

[34] Tang, Q.-Y., Zhang, Z., Xia, J., Ren, D., & Logothetis, D. E. (2010). Phosphatidylinositol 4,5-Bisphosphate Activates Slo3 Currents and Its Hydrolysis Underlies the Epidermal Growth Factor-induced Current Inhibition. Journal of Biological Chemistry, 285(25), 19259–19266. https://doi.org/10.1074/jbc.M109.100156

[35] Rohacs, T., Lopes, C. M. B., Jin, T., Ramdya, P. P., Molnar, Z., & Logothetis, D. E. (2003). Specificity of activation by phosphoinositides determines lipid regulation of Kir channels. Proceedings of the National Academy of Sciences, 100(2), 745–750. https://doi.org/10.1073/pnas.0236364100

[36] Balla, T. (2013). Phosphoinositides: Tiny Lipids With Giant Impact on Cell Regulation. Physiological Reviews, 93(3), 1019–1137. https://doi.org/10.1152/physrev.00028.2012

[37] Rjasanow, A., Leitner, M. G., Thallmair, V., Halaszovich, C. R., & Oliver, D. (2015). Ion channel regulation by phosphoinositides analyzed with VSPs—PI(4,5)P$_2$ affinity, phosphoinositide selectivity, and PI(4,5)P$_2$ pool accessibility. Frontiers in Pharmacology, 6. https://doi.org/10.3389/fphar.2015.00127

[38] McCune, C. D., Chan, S. J., Beio, M. L., Shen, W., Chung, W. J., Szczesniak, L. M., … Berkowitz, D. B. (2016). "Zipped Synthesis" by Cross-Metathesis Provides a Cystathionine β-Synthase Inhibitor that Attenuates Cellular H_2S Levels and Reduces Neuronal Infarction in a Rat Ischemic Stroke Model. ACS Central Science, 2(4), 242–252. https://doi.org/10.1021/acscentsci.6b00019
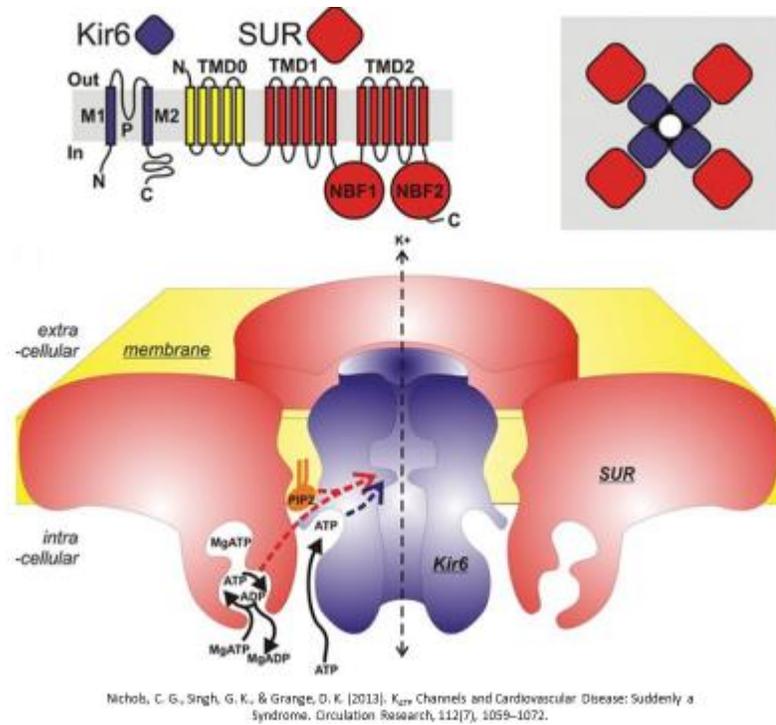
Nichols, C. G., Singh, G. K., & Grange, D. K. (2013). K_ATP Channels and Cardiovascular Disease: Suddenly a Syndrome. Circulation Research, 112(7), 1059–1072.

Figure 1

K*_{ATP} *Channel Subunits and Select Regulatory Factors: (Top left) schematic of one Kir6 and one SUR subunit of the K_ATP octamer, localized across a cellular membrane with "Out" and "In" used to mark extracellular and intracellular regions, respectively. For Kir6, the N-terminus, C-terminus, M1 and M2 membrane domains, and the P-loop gate are shown. In the Kir6.2Δ36 mutant, the last 36 amino acids of the C-terminus have been deleted. For SUR, the three transmembrane domains, TMD0, TMD1, and TMD2 are marked, along with the 2 nucleotide-binding folds, NBF1 and NBF2, as well as the N-terminus and C-terminus. (Top right) Shows a schematic of the basic organization of the octamer, with the four Kir6 pore-forming subunits surrounded by the four SUR subunits. (Bottom) Cutaway of the K_ATP octamer, showing half the channel, localized in a cellular membrane. Binding sites for ATP, ADP, MgATP, MgADP, and PIP₂ are shown, as well as the black dashed line in the center showing the permeation path of K⁺. Adapted from Nichols, C. G., Singh, G. K., & Grange, D. K. (2013). K_ATP Channels and Cardiovascular Disease: Suddenly a Syndrome. Circulation Research, 112(7), 1059–1072. https://doi.org/10.1161/CIRCRESAHA.112.300514.
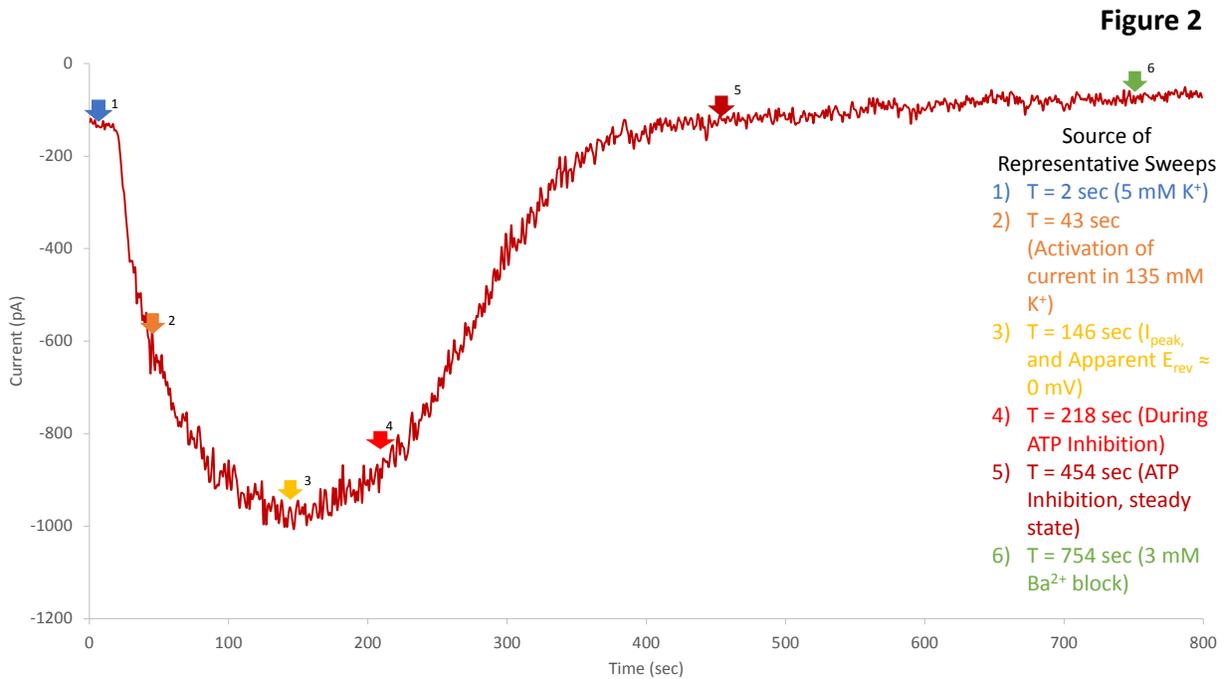
Figure 2

High ATP in the Patch Pipette Inhibits Kir6.2Δ36 Currents: Representative time course of whole-cell patch-clamp currents with HEK-293 cells transfected with Kir6.2Δ36 and recorded with 3 mM ATP in the patch pipette. Perfusion by the High-K$^+$ solution began at time = 10 sec and perfusion by the barium solution began at 700 sec. Colored arrows mark points corresponding to representative sweeps shown in Figure 3, with trace colors matching arrow colors. The inset legend is also color-matched to corresponding arrows, where blue is t = 2 sec, during perfusion by the Low-K$^+$ solution; orange is t = 43 sec, during activation by High-K$^+$ solution; yellow is t = 146 sec where I$_{MAX}$ occurs as well as the start of E$_{REV}$ ≈ 0; light-red is t = 218 sec, during ATP inhibition; dark-red is t = 454 sec, during ATP inhibition steady-state; and green is t = 754 sec, during perfusion by the barium solution. Pipette resistance = 7.1-7.3 MΩ. Series Resistance = 18.5 MΩ. Whole Cell Capacitance = 3.4 pF. Recording Resistance ≈ 1 GΩ.
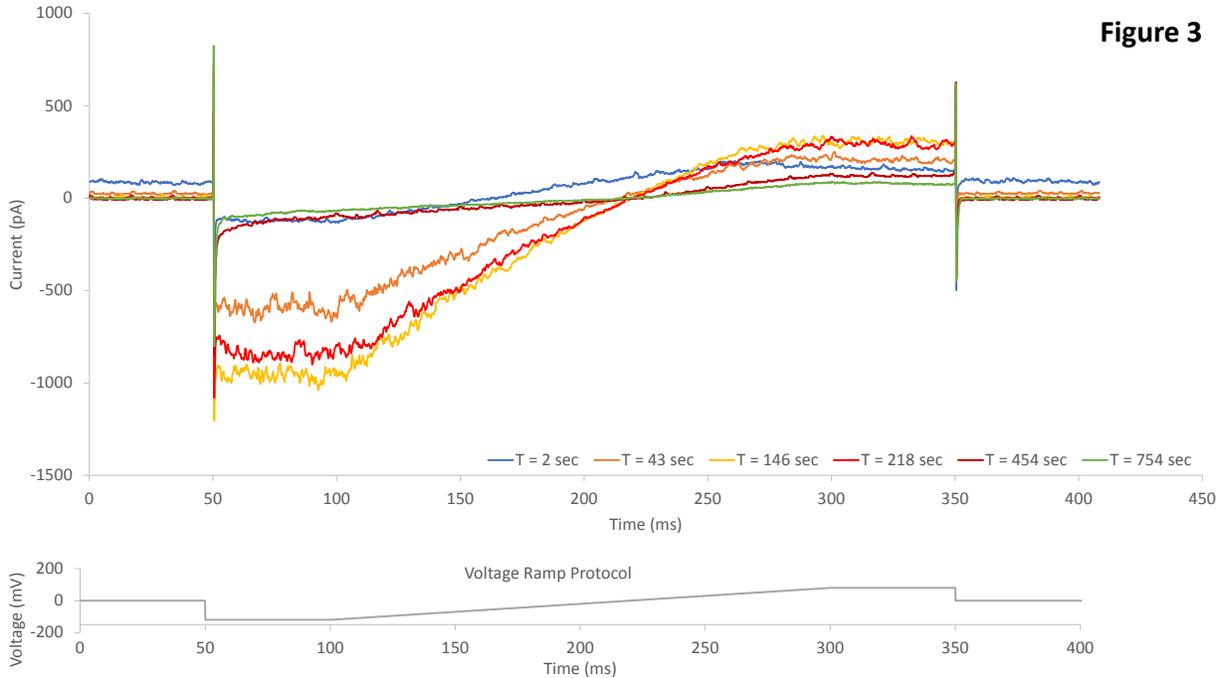
Figure 3

Representative Voltage-Ramp Current Sweeps from Time Course for Kir6.2Δ36 Inhibition by 3 mM ATP in the Patch Pipette: (Top) Color coded sweeps corresponding to colors and times from Figure 2, generated by the voltage-ramp protocol (bottom). The behavior of the channel with 3 mM ATP in the patch pipette first shows activation from increasing external K$^+$ concentration in the transition from the Low-K$^+$ to High-K$^+$ solutions, then inhibition after a sufficient concentration of ATP diffuses from the patch pipette into the cell. In this example, currents were inhibited to the point where the perfusion of the barium solution contributes negligibly to further inhibition. (Bottom) Voltage-ramp protocol – each sweep is 1 sec, with times not shown being at the holding potential of 0 mV. From left to right, t = 0 – 50 ms are at 0 mV; t = 50 – 100 ms of -120 mV; t = 100 – 300 ms is a linear increase in voltage from -120 mV to +80 mV; and t = 350 – 400 ms holds at 0 mV.
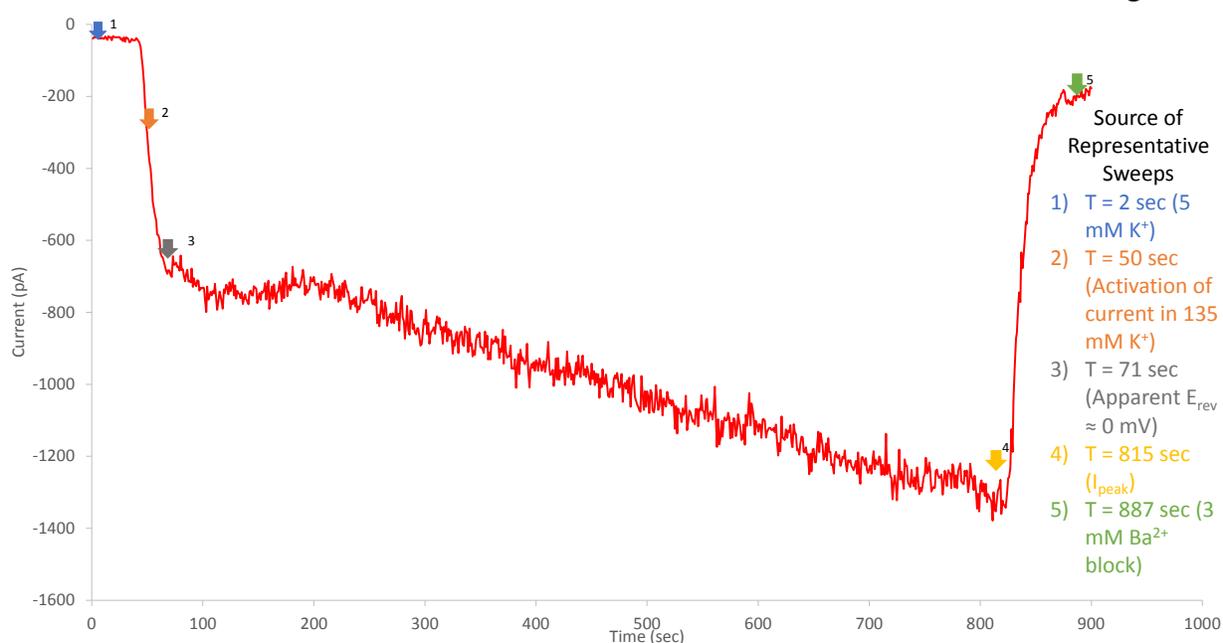
Figure 4

Figure 4

0.3 mM ATP in the Patch Pipette Permits Rather than Inhibits Kir6.2Δ36 Currents:
Representative time course of whole-cell patch-clamp currents with HEK-293 cells
transfected with Kir6.2Δ36, recorded with 0.3 mM ATP in the patch pipette. Perfusion
by the High-K+ solution began at t = 19 sec and perfusion by the barium solution began
at 790 sec. Colored arrows mark points from which representative sweeps are taken
and shown Figure 5, with trace colors matching arrow colors. The inset legend is also
color-matched to corresponding arrows, where blue is t = 2 sec, during perfusion by the
Low-K+ solution; orange is t = 50 sec, during activation in the High-K+ solution; grey is t
= 71 sec where $E_{REV} ≈ 0$; yellow is t = 815 sec, at the point of I_{MAX}; and green is t = 887
sec, during perfusion by the barium solution, while in steady-state inhibition. Pipette
resistance = 5.0-5.2 MΩ. Series Resistance = 12.5 MΩ. Whole Cell Capacitance =
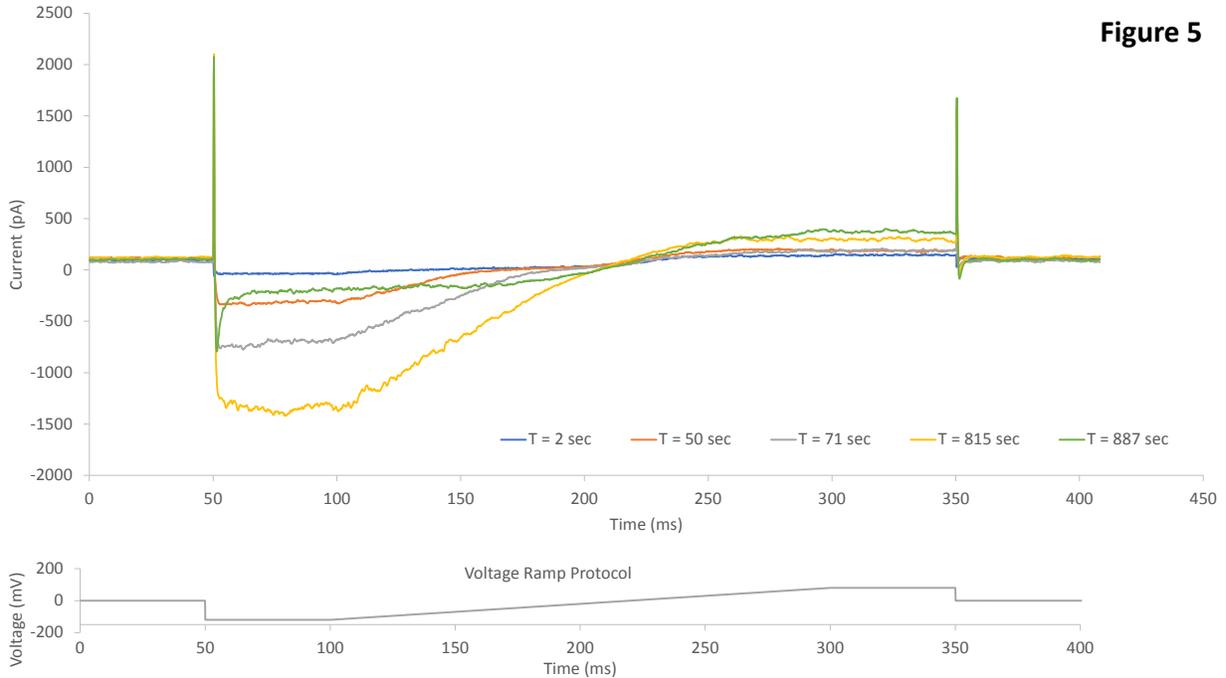32.9 pF. Recording Resistance ≈ 0.5 GΩ.

Figure 5

***Representative Voltage-Ramp Current Sweeps from Time Course for Kir6.2Δ36
with 0.3 mM ATP in the Patch Pipette***: (Top) Color coded sweeps corresponding to
colors and times from Figure 4, generated by the voltage-ramp protocol (bottom). The
behavior of the channel with 0.3 mM ATP goes as anticipated, showing activation by
increasing K^+ concentration in the transition from the Low-K^+ to High-K^+ solutions, then
maintains an environment permissive to the activated currents as ATP diffuses from the
pipette into the cell, then the currents are inhibited by perfusion of the barium solution.
(Bottom) Voltage-ramp protocol – each sweep is 1 sec, with times not shown being at
the holding potential of 0 mV. From left to right, t = 0 – 50 ms are at 0 mV; t = 50 – 100
ms of -120 mV; t = 100 – 300 ms is a linear increase in voltage from -120 mV to +80
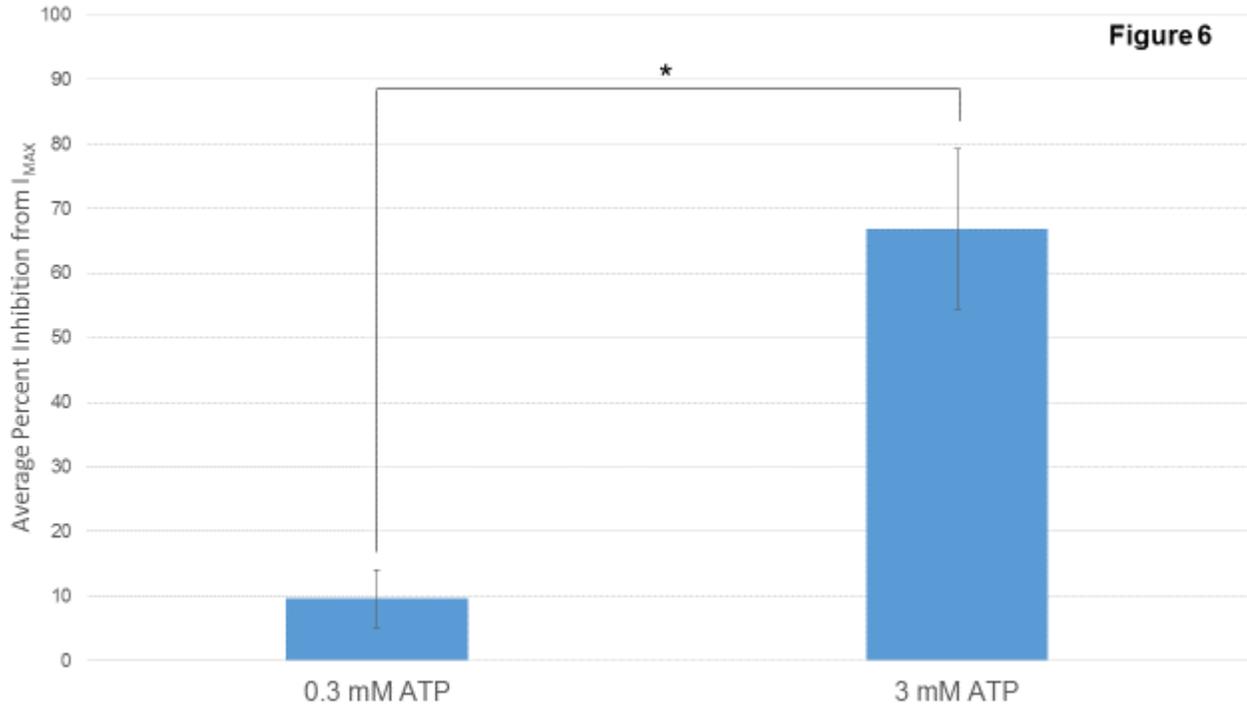mV; and t = 350 – 400 ms holds at 0 mV.

Figure 6

Effects of 0.3 mM Compared to 3 mM ATP on Kir6.2Δ36 Currents: Whole-cell patch-clamp inward currents from HEK293 cells transfected with Kir6.2Δ36, generated in the presence of either 0.3 mM or 3 mM ATP in the patch pipette (representative traces shown in Figures 2-4), were collected and analyzed. From each run, the percent inhibition from the maximum inward current (I_{MAX}) to the average of currents generated from the 11 sec before the start of perfusion by the barium solution. The averages of these percent inhibitions are presented here. The average percent inhibition for 0.3 mM ATP was 9.6% +/- 4.4% (SEM), n = 6. A 1-sample t-test was performed to test H_0: $\mu = 0$ against H_A: $\mu \neq 0$, and found that this average was not statistically different from 0%, p-value = 0.084. The average percent inhibition for 3 mM ATP was 67% +/- 12% (SEM), n = 5. A 1-sample t-test was performed to test H_0: $\mu = 0$ against H_A: $\mu > 0$, and found the average inhibition to be statistically greater than 0%, p-value = 0.003. A one-tailed Mann-Whitney U test analysis was performed to test the H_0 that the two concentrations did not result in statistically distinct inhibitions from I_{MAX}, against the H_A that 3 mM ATP results in greater inhibitions from I_{MAX} than 0.3 mM ATP, and found that 3 mM ATP results in significantly greater inhibitions, p-value = 0.003. * indicates p<0.05.

Figure 7

*5-ptase + CIBN-CAAX Light-Stimulation Showing Large Inhibition of Kir2.3 Currents***:** Representative time course of whole-cell patch-clamp currents with HEK-293 cells transfected with Kir2.3, the 5-ptase, and CIBN-CAAX, with 0.3 mM ATP in the patch pipette. Perfusion by the High-K^+ solution began at t = 10 sec; light-stimulation of the phosphatase system began at t = 150 sec (marked by vertical blue line); and inhibition from the resulting depletion of PIP_2 proceeds until reaching a steady-state, at which point the barium solution perfusion was started (t = 250 sec). The voltage-ramp protocol used was identical to the one shown in Figures 3 and 5. Pipette resistance = 6.1-6.3 MΩ. Series Resistance = 19.3 MΩ. Whole Cell Capacitance = 13.9 pF. Recording Resistance ≈ 1 GΩ.
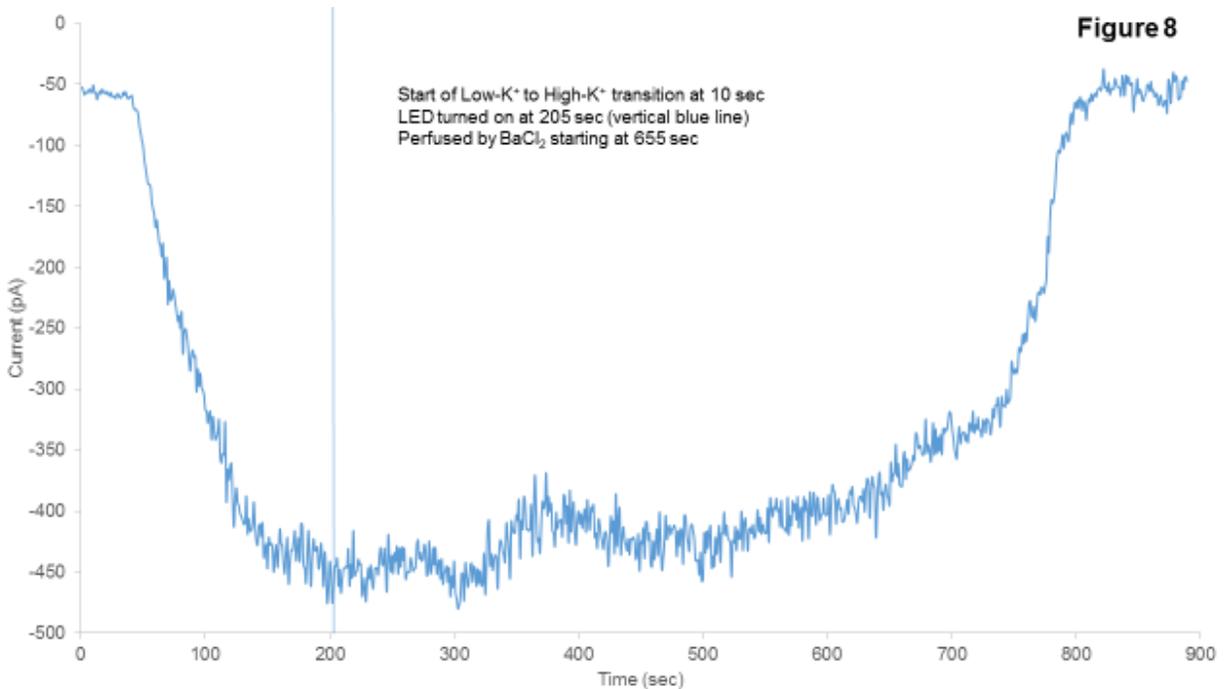
Figure 8

5-ptase + CIBN-CAAX Light-Stimulation Shows No Observable Rapid Inhibition of Kir6.2Δ36 Currents: Representative time course of whole-cell patch-clamp currents with HEK-293 cells transfected with Kir6.2Δ36, the 5-ptase, and CIBN-CAAX, with 0.3 mM ATP in the patch pipette. Perfusion by the High-K$^+$ solution began at t = 10 sec; light-stimulation began at t = 205 sec (marked by vertical blue line); no observable rapid change in the behavior of the currents occurred after light-stimulation, but signs of long-term inhibition were apparent; and perfusion by the barium solution began at t = 655 sec. The voltage-ramp protocol used was identical to the one shown in Figures 3 and 5. Pipette resistance = 7.6-7.8 MΩ. Series Resistance = 15.1 MΩ. Whole Cell Capacitance = 20.8 pF. Recording Resistance ≈ 1 GΩ.
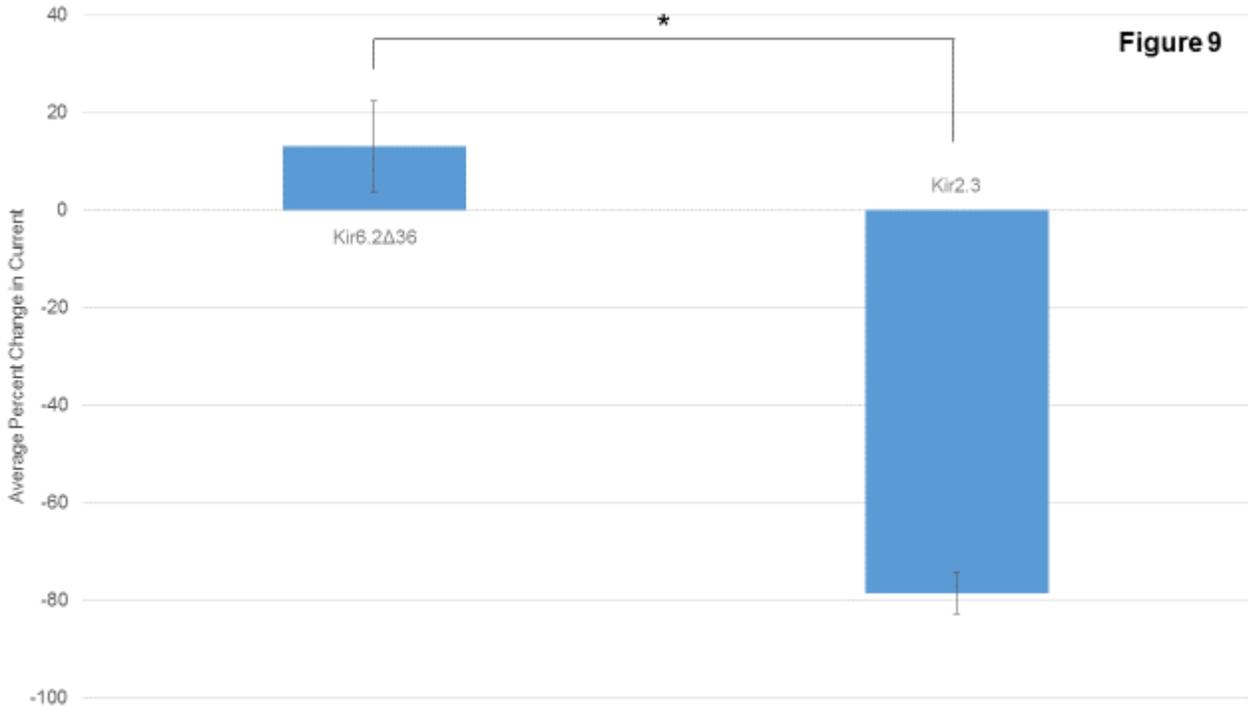
Figure 9

Average Percent Change in Currents by 5-ptase + CIBN-CAAX Light-Stimulation for Kir6.2Δ36 Compared to Kir2.3: Whole-cell patch-clamp inward currents comparing the average of currents over 11 sec before the light-stimulation to the average of currents over 11 sec before beginning the barium solution perfusion, which corresponds to the steady-state after changes in currents, were collected and analyzed to find a percent change for each run. These percent changes were averaged and are shown here. For Kir6.2Δ36, the current showed an average percent change of +13% +/- 9.4% (SEM), n = 13. A 1-sample t-test was performed to test H_0: $\mu = 0$ against H_A: $\mu \neq 0$, and found that this average was not statistically different from 0%, p-value = 0.189. For Kir2.3, the currents showed an average percent change of -79% +/- 4.3% (SEM), n = 6. A 1-sample t-test was performed to test H_0: $\mu = 0$ against H_A: $\mu > 0$, and found that this average inhibition was statistically greater than 0%, p-value < 0.001. A two-tailed Mann-Whitney U test analysis was performed to test the H_0 that the light-stimulated 5-ptase system had a statistically similar long-term effect on both channels, against the H_A that, although similarly activated by PIP_2, the channels had statistically distinct responses, giving a p-value < 0.001. * indicates p<0.05.
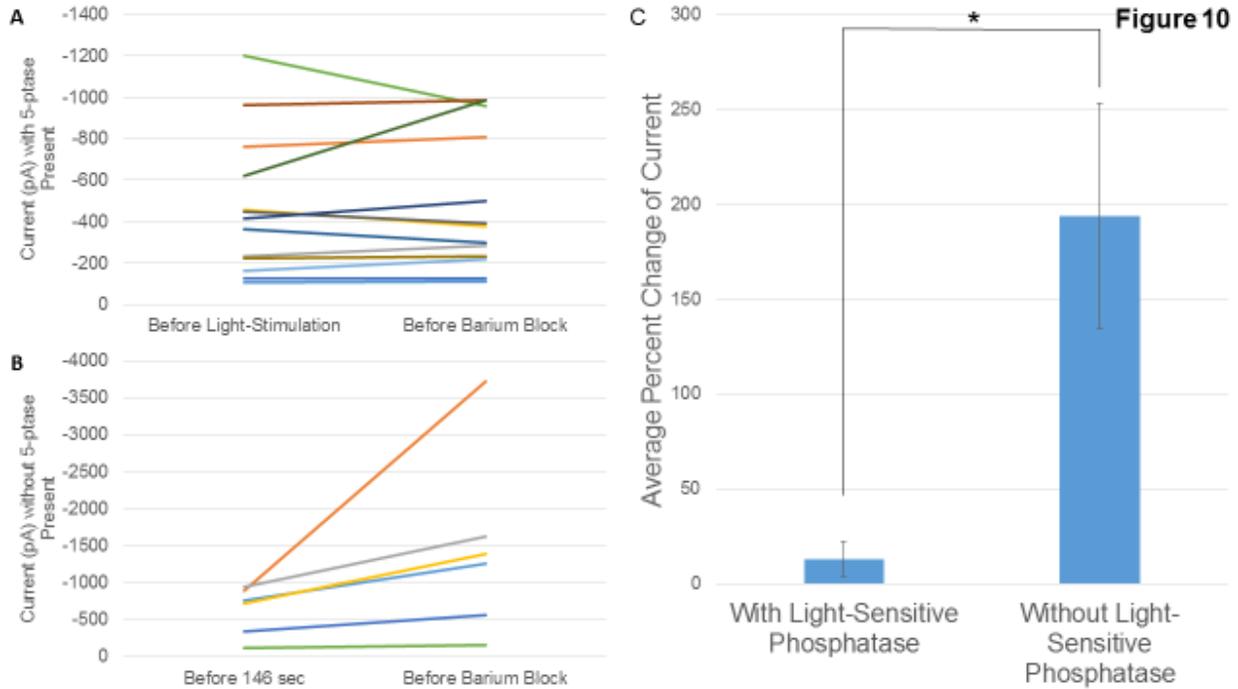
36

Figure 10

Effects of 0.3 mM ATP in the Patch Pipette on Kir6.2Δ36 Currents, with and without 5-ptase + CIBN-CAAX: In order to determine if the light-stimulation of the 5-ptase system had a significant long-term impact on Kir6.2Δ36 currents, data from cells transfected with the channel, and with 0.3 mM ATP in the patch pipette, were analyzed to compare between those co-transfected with the 5-tase system and those without. **A**) Colored lines connect data points from the same run, representing the average of currents over 11 sec before light-stimulation to the average of currents over the 11 sec before perfusion by the barium solution for co-transfected cells. **B**) Since no light-stimulation was attempted in runs without the 5-ptase present, the average start of light-stimulation from the co-transfected data set (t = 146 sec) was used to analyze data generated without, and otherwise the analysis was performed as in Figure 10A. **C**) The average of the percent changes found for each run with the 5-ptase system, and its statistical test, is the same as presented in Figure 9 (+13% +/- 9.4% (SEM), n = 13, p = 0.189). Without the system, the average change was +190% +/- 59% (SEM), n = 6. A 1-sample t-test was performed to test H_0: $\mu = 0$ against H_A: $\mu > 0$, and found that this average was statistically greater than 0%, p-value = 0.011. A two-tailed Mann-Whitney U test analysis was performed to test the H_0 that the light-stimulation of the phosphatase system, in the presence of 0.3 mM ATP, had a statistically similar effect as 0.3 mM ATP alone, against the H_A that its light-stimulation had a significant long-term impact on Kir6.2Δ36 currents, giving a p-value = 0.001. * indicates p<0.05.
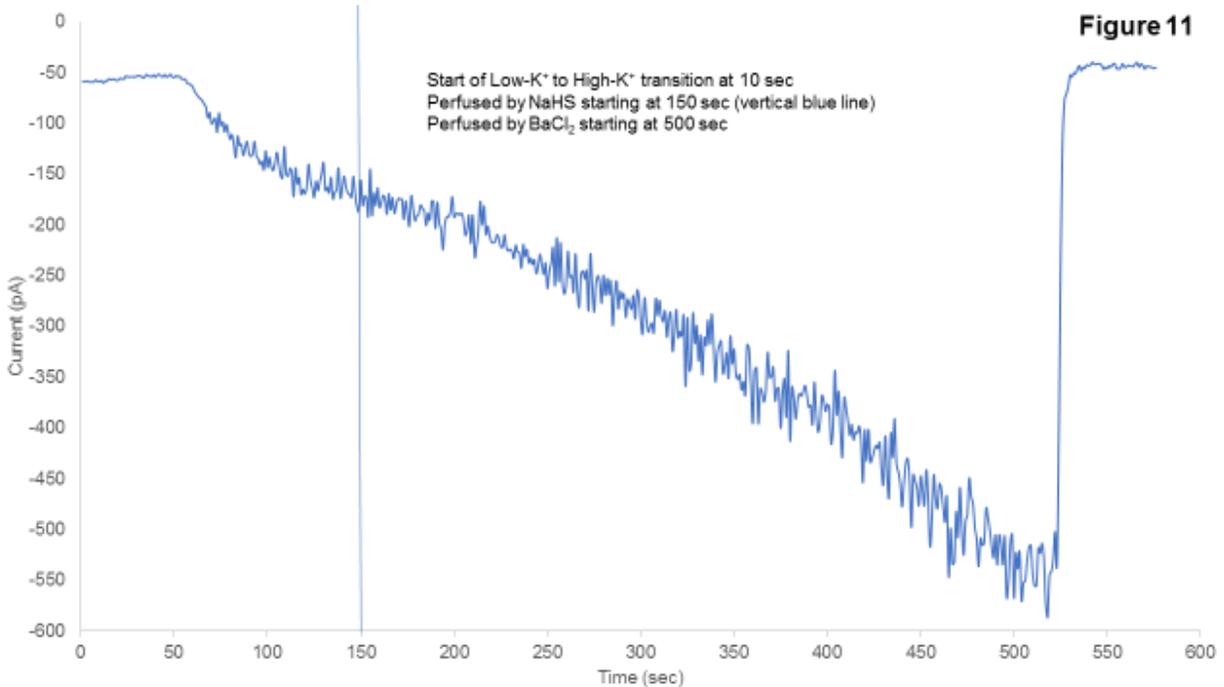
Figure 11

Start of Low-K⁺ to High-K⁺ transition at 10 sec
Perfused by NaHS starting at 150 sec (vertical blue line)
Perfused by BaCl₂ starting at 500 sec

Figure 11

Activation of Kir6.2Δ36 Currents by Perfusion of 3 mM NaHS without DiC₈:
Representative time course of whole-cell patch-clamp inward currents with HEK-293
cells transfected with Kir6.2Δ36, with 0.3 mM ATP in the patch pipette. Perfusion by the
High-K⁺ solution began at t = 10 sec; perfusion by the NaHS solution began at t = 150
sec (marked by vertical blue line); and perfusion by the barium solution began at t = 500
sec. The voltage-ramp protocol used was identical to the one shown in Figures 3 and 5.
Pipette resistance = 4.7-4.9 MΩ. Series Resistance = 24.1 MΩ. Whole Cell
Capacitance = 14.0 pF. Recording Resistance ≈ 1 GΩ.

The graph shows the following annotations:

Start of Low-K⁺ to High-K⁺ transition at 10 sec
Perfused by NaHS starting at 250 sec (vertical blue line)
Perfused by BaCl₂ starting at 500 sec

Figure 12

Y-axis: Current (pA), ranging from 0 to -1600
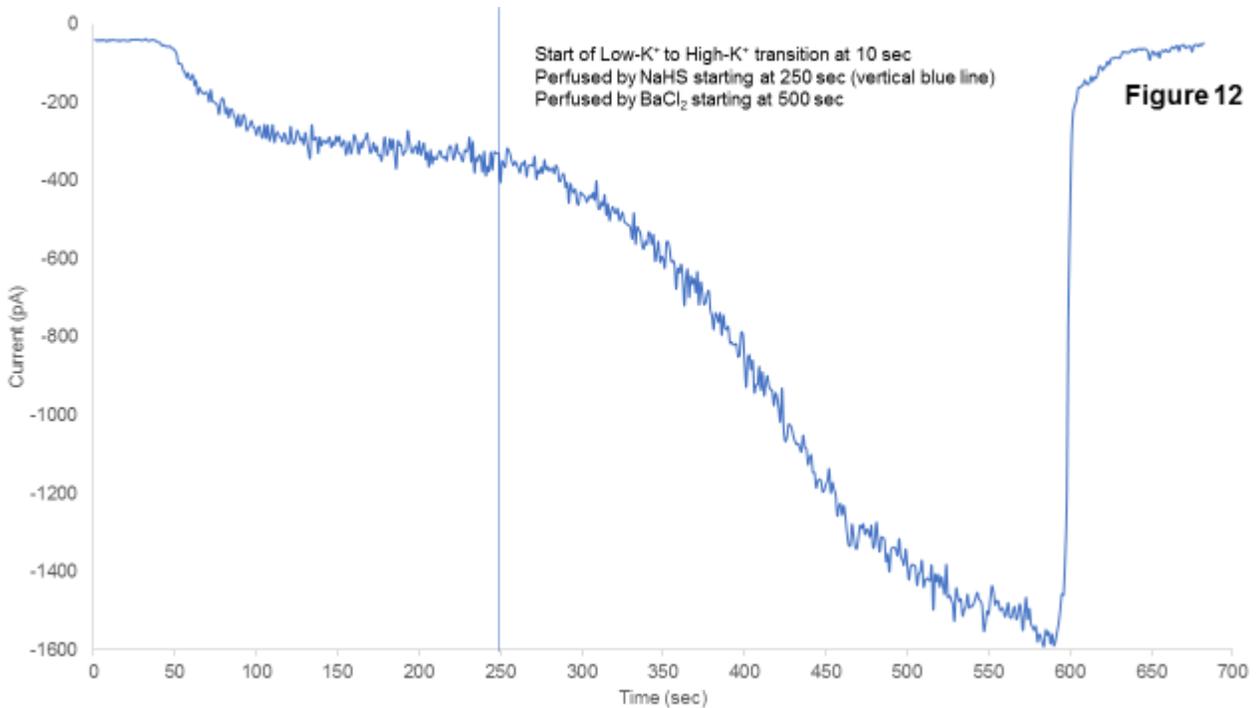X-axis: Time (sec), ranging from 0 to 700

Figure 12

Activation of Kir6.2Δ36 Currents by Perfusion of 3 mM NaHS with 0.2 mM DiC₈ in the Patch Pipette: Representative time course of whole-cell patch-clamp inward currents with HEK-293 cells transfected with Kir6.2Δ36, with 0.3 mM ATP and 0.2 mM DiC₈ in the patch pipette. Perfusion by the High-K⁺ solution began at t = 10 sec; perfusion by the NaHS solution began at t = 250 sec (marked by vertical blue line); and perfusion by the barium solution began at t = 500 sec. The voltage-ramp protocol used was identical to the one shown in Figures 3 and 5. Pipette resistance = 4.6-4.8 MΩ. Series Resistance = 47.2 MΩ. Whole Cell Capacitance = 13.0 pF. Recording Resistance ≈ 1 GΩ.
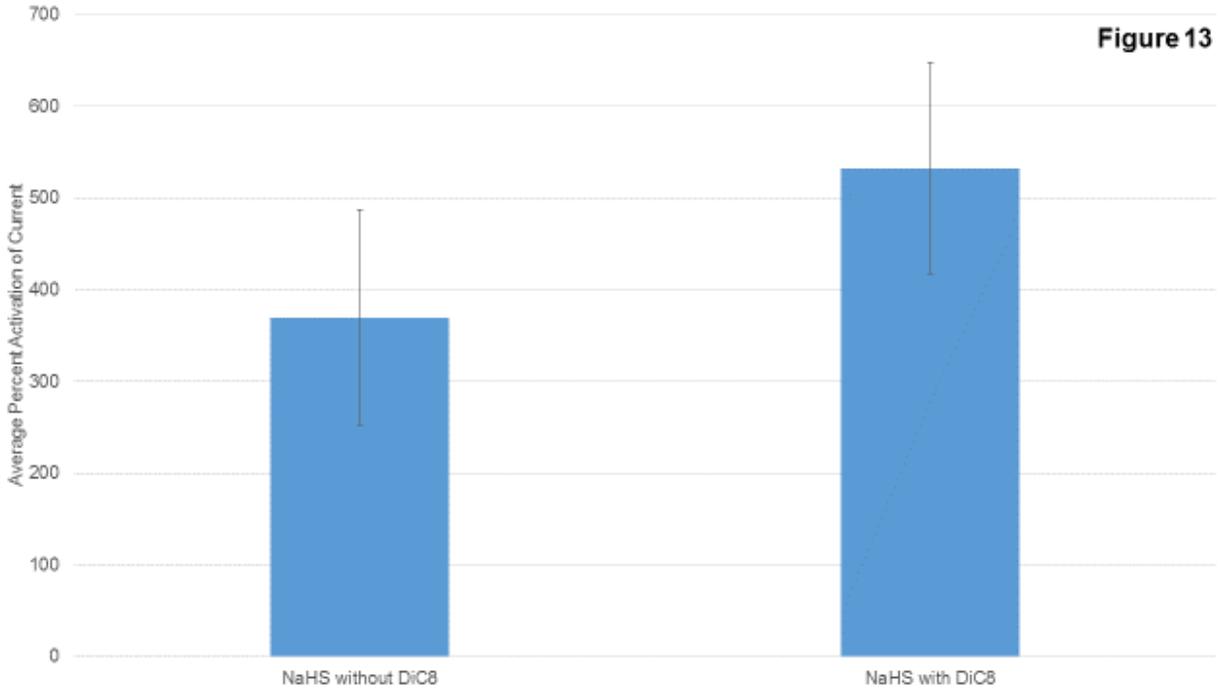
Figure 13

Average Percent Change of Kir6.2Δ36 Currents by Perfusion of 3 mM NaHS with and without 0.2 mM DiC8 in the Patch Pipette: Analysis of whole-cell patch-clamp inward currents comparing the average of currents over 11 sec before the start of perfusion of NaHS to the average of currents over 11 sec before the start of perfusion by the barium solution, which corresponds to the steady-state after changes in currents, gave a percent activation for each run. These percent activations were averaged and are shown here. Without the presence of DiC_8 in the patch pipette, the currents showed an average percent activation of 370% +/- 120% (SEM), n = 6. A 1-sample t-test was performed to test H_0: $\mu = 0$ against H_A: $\mu > 0$, and found that this average was statistically greater than 0%, p-value = 0.013. Without the presence of DiC_8, the currents showed an average percent activation of 530% +/- 120% (SEM), n = 6. A 1-sample t-test was performed to test H_0: $\mu = 0$ against H_A: $\mu > 0$, and found that this average was statistically greater than 0%, p-value = 0.003. A one-tailed Mann-Whitney U test analysis was performed to test the H_0 that there was no difference between activating effects of NaHS in the presence of 0.2mM DiC_8 in the patch pipette to without it, to the H_A that the presence of DiC_8 increased these activating effects, giving a p-value = 0.087.